using a theory developed by Höck et al.,[15] in terms of site entropy and E_{1g} and E_{2g} strain components. Variable-temperature EPR experiments are under way to try to identify the nature of the disorder.

The low-temperature phase can be characterized by stating that the disorder resulting from the entropy mentioned above (the energy gain of which decreases when the temperature is lowered) is overruled by energy gain that results from fixing the Jahn-Teller elongation at the bottom of the wells of the warped potential energy surface, the so-called Mexican hat. This mechanism also prevents incommensurability but does not explain the 5-fold unit cell.

Recently some authors[3] have tried to describe this kind of Jahn-Teller system with a pseudospin model as mentioned in the Introduction. Concerning the intermediate phase of both $RbCrCl_3$ and TMCuC, it is more difficult to imbed those in a pseudospin Ising system since this model does not allow for self-entropy of the Cu site. This fact makes it impossible to describe the successive transitions in TMCuC in the light of a "devil's staircase" as formulated by, e.g., Bak[16] for magnetic spins. Another model, the ANNNI model,[17] applied to $CsCuCl_3$ and the low-temperature TMCuC reveals that the ordering of the Jahn-Teller-elongated axes in the former compound is much more stable, by a factor of 5, than the one found in TMCuC. This model can therefore not explain this low-temperature structure. This in fact does not surprise us, as it is shown in a recent paper by Maaskant and Haije[18] that apart from the usual quadrupolar deformations, due to the Jahn-Teller effect, also dipolar distortions and their mutual interactions have to be taken into account. This would lead, in the case of TMCuC, to a complicated pseudospin-phonon coupling scheme. Furthermore, the low-temperature structure described in this paper is not the $T = 0$ K structure. Recent magnetic measurements on a single crystal of TMCuC revealed a phase transition at about 140 K. X-ray experiments showed the crystal to transform to a multidomain structure. Neutron diffraction experiments will be carried out in the near future to determine this crystal phase.

Acknowledgment. The support of NSF Grant CHE-8408407 and of The Boeing Co. in the establishment of the X-ray diffraction facility at Washington State University is gratefully acknowledged, as is the support of the donors of the Petroleum Research Fund, administered by the American Chemical Society. The investigations were supported in part (W.G.H.) by the Netherlands Foundation for Chemical Research (SON) with financial aid from the Netherlands Organization for the Advancement of Pure Research (ZWO). The Netherlands Organization for the Advancement of Pure Research is acknowledged for a visiting professorship for R.D.W.

Registry No. $(CH_3)_4NCuCl_3$, 58428-65-2.

Supplementary Material Available: Tables of anisotropic thermal parameters for $(CH_3)_4NCuCl_3$ at 213, 323, and 405 K and hydrogen atom coordinates for $(CH_3)_4NCuCl_3$ at 213 and 323 K (5 pages); tables of observed and calculated structure factors for $(CH_3)_4NCuCl_3$ at 213, 323, and 405 K (27 pages). Ordering information is given on any current masthead page.

(15) Höck, K.; Schröder, G.; Thomas, H. *Z. Phys. B: Condens. Matter Quanta* **1978**, *30*, 403.
(16) Bak, P. In *Recent Developments in Condensed Matter Physics*; De Vreese, J. T., Ed.; Plenum: New York, 1981; Vol. I, p 489.
(17) Fisher, M. E.; Selke, W. *Philos. Trans. R. Soc. London, A* **1981**, *302*, 1.
(18) Maaskant, W. J. A.; Haije, W. G. *J. Phys. C* **1986**, *19*, 5295.

Contribution from the Department of Physics, Clark University, Worcester, Massachusetts 01610, and Department of Chemistry, Washington State University, Pullman, Washington 99164

Alternating Exchange in Homonuclear Ferrimagnetic Linear Chains. Tetrakis(tetramethylene sulfoxide)copper(II) Hexahalodicuprate(II) (Halo = Chloro, Bromo): Crystal Structures and Magnetic Susceptibilities

C. P. Landee,*† A. Djili,† D. F. Mudgett,† M. Newhall,† H. Place,‡ B. Scott,‡ and R. D. Willett*‡

Received September 4, 1987

The two compounds $\{Cu(TMSO)_4\}[Cu_2X_6]$ (X = Br (**1**) and Cl (**2**); TMSO = tetramethylene sulfoxide) have been synthesized and their crystal structures determined at room temperature. They are isostructural, and both crystallize in the triclinic system, space group $P\bar{1}$, with cell parameters for **1** of $a = 8.448$ (2) Å, $b = 9.630$ (2) Å, $c = 11.655$ (2) Å, $\alpha = 65.42$ (1)°, $\beta = 71.59$ (2)°, and $\gamma = 73.52$ (1)°. The cell parameters of **2** are $a = 8.250$ (4) Å, $\beta = 9.330$ (5) Å, $c = 11.131$ (6) Å, $\alpha = 67.59$ (4)°, $\beta = 73.29$ (6)°, and $\gamma = 74.67$ (6)°. The structures consist of alternating chains of dimeric $Cu_2X_6^{2-}$ anions and monomeric $Cu(TMSO)_4^{2+}$ cations extended along the c axes. The magnetic properties have been investigated down to 1.4 K. Both compounds show evidence of two types of magnetic interactions: ferromagnetic exchange within the dimeric units ($J_d(Br)/k = 12$ (4) K, **1**; $J_d(Cl)/k = 20$ (5) K, **2**) and a weaker exchange between the dimeric and monomeric copper atoms that is antiferromagnetic for **1** ($J_m(Br)/k = -1.5$ K) and ferromagnetic for **2** ($J_m(Cl)/k = 1.6$ K). The magnetic susceptibility of the bromide salt, **1**, is interpreted in terms of a ferrimagnetic linear-chain model where the ferrimagnetism of the homometallic system arises from an odd number of magnetic atoms per unit cell. The corresponding chloride salt, **2**, represents a ferromagnetic chain, with no evidence of any antiferromagnetic interchain coupling observable down to the lowest temperature measured.

Introduction

The discovery of ordered, bimetallic linear chains[1] has opened up new possibilities in magnetochemistry. These materials consist of two different transition-metal ions bridged by either carboxylate groups[2] or substituted oxalate groups[3-5] in a ...-M-L-M'-L-M-... pattern and thus permit the magnetic pairing of a wide variety of metal ions. The magnetic interactions have inevitably been found to be antiferromagnetic, but the anisotropy of the superexchange is controlled by the specific ions involved: the behavior of the Co^{2+} ion is always best described by the anisotropic Ising model,[6] while Mn^{2+}, Ni^{2+}, and Cu^{2+} systems have been modeled

* To whom correspondence should be addressed.
† Clark University.
‡ Washington State University.

(1) For a review, see: Landee, C. P. In *Organic and Inorganic Low Dimensional Crystalline Materials*; Drillon, M., Delhaes, P., Eds.; NATO ASI Series; Plenum: New York; in press.
(2) Beltran, D.; Escriva, E.; Drillon, M. *J. Chem. Soc., Faraday Trans. 2* **1982**, *78*, 1773.
(3) Gleizes, A.; Verdaguer, M. *J. Am. Chem. Soc.* **1984**, *106*, 3727.
(4) Verdaguer, M.; Julve, M.; Michalowicz, A.; Kahn, O. *Inorg. Chem.* **1983**, *22*, 2624.
(5) Pei, Y.; Verdaguer, M.; Kahn, O.; Sletten, J.; Renard, J.-P. *Inorg. Chem.* **1987**, *26*, 138.
(6) Georges, R.; Curély, J.; Drillon, M. *J. Appl. Phys.* **1985**, *58*, 914.

0020-1669/88/1327-0620$01.50/0

with the isotropic Heisenberg model.[7] Their characteristic magnetic behavior arises from the failure of the antiferromagnetic exchange to completely cancel the different moments of the adjacent metal ions; at low temperatures, a net, uncompensated moment remains within each unit cell. The product χT of such materials first decreases upon cooling from high temperatures, displays a minimum at an intermediate temperature that depends on the interaction strength J as well as the spin values of the two metal ions, and then diverges at low temperature.[8] The divergence is due to the remaining, uncompensated moments within each unit cell aligning in a "ferromagnetic-like" pattern.

The ordered bimetallic ferrimagnets are currently under study as a means of obtaining magnets with ground states containing spontaneous moments. While many examples exist of linear-chain compounds with ferromagnetic interchain interactions,[9,10] every such system has been found to order in an antiferromagnetic ground state with no spontaneous moment. Pei et al.[11] have recently reported on the bimetallic chain $MnCu(pbaOH)(H_2O)_3$, where pbaOH denotes 1,3-propanediylbis(oxamato) with the central methylene group of the 1,3-propanediyl chain replaced by CHOH. This compound, whose ferrimagnetic chains are nearly identical with those in $MnCu(pba)(H_2O)_3 \cdot 2H_2O$ reported earlier,[5] nevertheless achieves a state of spontaneous order at 4.6 K, while the pba compound undergoes a transition to a Néel state at 2.2 K. The important structural difference between the two compounds is the relative position of adjacent chains. While the chains in the pba compound are simply separated by one unit cell normal to the chains, adjacent chains in the pbaOH compound are displaced by nearly half of a repeat unit parallel to the chains. Such a displacement has the effect of providing an interchain interaction between Mn^{2+} on one chain and Cu^{2+} on the next. This Mn^{2+}–Cu^{2+} exchange is always antiferromagnetic and ensures that the net moments on all chains are parallel.

Ferrimagnetism has the potential of arising from several different origins, although every one-dimensional ferrimagnet reported to date originates in ordered bimetallic systems. A homometallic chain can also be ferrimagnetic, provided alternating sites exist within the chain, which create alternating g factors and therefore alternating moments. This possibility was recognized in the study[12] of $Ni_2(EDTA)(H_2O)_4 \cdot 2H_2O$, but the data did not extend to sufficiently low temperatures to confirm the predicted divergence in susceptibility. Ferrimagnetism can also arise in a (homo- or heterometallic) system that contains an odd number of metallic sites per unit cell. Even when the moments on each site are identical, the odd number present ensures that there will remain an uncompensated moment within each unit cell. If the adjacent net moments couple in a ferromagnetic manner, ferrimagnetism arises at low temperatures. In this paper, we report the structures and magnetic properties of two such homometallic ferrimagnetic linear chains,[13] tetrakis(tetramethylene sulfoxide)copper(II) hexahalodicuprate(II) (halo = chloro, bromo): $[Cu(TMSO)_4][Cu_2X_6]$. For simplicity, we shall refer to these compounds as $CuX_2 \cdot {}^4/_3TMSO$.

Experimental Section

Syntheses. The bromide compound was originally prepared by dissolving 4.3 g (1.9 mol%) of copper bromide in absolute ethanol and then adding dropwise an equimolar allotment of the TMSO. The solution was stirred for 2 h at room temperature and then placed in a desiccator. After several days, well-shaped black prismatic crystals were formed. Upon crushing, the powder also appears black. The composition was verified by commercial chemical analysis.[14] Anal. calcd for $C_{16}H_{32}S_4O_4Cu_3Br_6$: C, 17.68; H, 2.97; O, 5.89; S, 11.80; Cu, 17.54; Br, 44.12. Found: C, 17.80; H, 2.87; O, 5.18; S, 12.71; Cu, 17.54; Br, 43.91. The magnetic study and chemical analysis were conducted on the same batch. The X-ray analysis was conducted on a crystal obtained from a different batch that was formed from room-temperature evaporation of 95% ethanolic solutions of mixtures of copper bromide and TMSO in a $1:{}^4/_3$ mole ratio. The identity of the magnetic and X-ray batches has been confirmed by comparison of powder X-ray patterns.

It has been found that strict stoichiometry is not necessary for the production of the 4:3 bromide phase when absolute or 95% ethanol or propanol is used. When methanol is used as a solvent, the bis form is favored as reported previously.[15] The bis phase is readily distinguished as the crystals of $CuBr_2 \cdot 2TMSO$ are dark green and crush to a light yellow-green powder. A third, red phase has been found to grow out of 2-propanol. It has been identified as $Cu_4Br_6O(TMSO)_4$, a tetrameric copper cluster, which has been previously reported.[16]

The chloride analogue was prepared by dissolving anhydrous copper chloride in methanol and stirring in an amount of TMSO in slight excess of the stoichiometric amount. Large red crystals with well-developed faces appeared after several days of slow evaporation. The crystals are distinguished from the needlelike mono phase,[17] $CuCl_2 \cdot TMSO$, both by the crystal habit and by the red-green pleochroism evident in unpolarized light. The 4:3 phase is readily prepared from methanol or ethanol but is not formed in other common alcohols. Attempts to prepare it in other solvents have always led to a combination of the mono phase and the green bis phase.[18] Anal. calcd for $C_{16}H_{32}S_4O_4Cu_3Cl_6$: C, 23.44; H, 3.93; O, 7.80; S, 15.64; Cu, 23.25; Cl, 25.94. Found:[14] C, 23.10; H, 3.95; O, 7.63; S, 16.08; Cu, 23.48; Cl, 25.82.

Crystallographic Data Collection and Structure Determination. X-ray diffraction data collections were performed on a Nicolet R3m/E diffractometer system,[19] and the structures were solved by using direct methods within the Version 4.1 SHELXTL structure solution package.[20] As shown in Table I, $CuBr_2 \cdot {}^4/_3TMSO$ is triclinic $P\bar{1}$, with $a = 8.448$ (2) Å, $b = 9.630$ (2) Å, $c = 11.655$ (2) Å, $\alpha = 65.42$ (1)°, $\beta = 71.59$ (2)°, $\gamma = 73.52$ (1)°, and $Z = 1$ for $\rho_{calcd} = 2.22$ g cm^{-3}. An empirical absorption correction ($\mu = 96.18$ cm^{-1}) was applied for the room-temperature data collection. The structure was solved via direct methods, which revealed a copper atom on a special position and a second copper atom near three bromine atoms. Subsequent difference maps revealed the positions of all the other non-hydrogen atoms. Hydrogen atoms were fixed at calculated positions ($r_{C-H} = 0.96$ Å). A least-squares refinement on 152 parameters achieved a final R value of 0.0353, with $R_w = 0.0403$. The thermal parameters were anisotropic on all non-hydrogen atoms, while the hydrogen atom isotropic thermal parameters were fixed at 0.10, a value approximately 20% larger than those of the corresponding heavy atom. The largest peak on the final difference map had a residual electron density of 0.62 e Å^{-3}, near Br(3). Atomic coordinates and thermal parameters are given in Table II, and bond distances and angles, in Table IV.

The chloride analogue, $CuCl_2 \cdot {}^4/_3TMSO$, is likewise triclinic $P\bar{1}$, with $a = 8.250$ (4) Å, $b = 9.330$ (5) Å, $c = 11.131$ (6) Å, $\alpha = 67.59$ (4)°, $\beta = 73.29$ (6)°, $\gamma = 74.67$ (6)°, and $Z = 1$ for $\rho_{calcd} = 1.82$ g cm^{-3} (Table I). Empirical absorption corrections ($\mu = 29.58$ cm^{-1}) have been made with an ellipsoidally shaped crystal assumed. Two standards were monitored every 100 reflections. The structure was solved in the same manner used for the bromide; refinement on 152 parameters gave final values of $R = 0.0377$ and $R_w = 0.0456$. The largest peak on the final difference map had a residual electron density of 0.7 e Å^{-3}, near Cl(3). Atomic coordinates and thermal parameters are given in Table III, and bond distances and angles, in Table V. Tables of anisotropic thermal parameters and hydrogen atom coordinates plus observed and calculated

(7) Drillon, M.; Coronado, E.; Beltran, D.; Curély, J.; Georges, R.; Nugteren, P. R.; de Jongh, L. J.; Genicon, J. L. *J. Magn. Magn. Mater.* **1986**, *54–57*, 1507.
(8) Curély, J.; Georges, R.; Drillon, M. *Phys. Rev. B: Condens. Matter* **1986**, *33*, 6243.
(9) Willett, R. D.; Gaura, R. M.; Landee, C. P. In *Extended Linear Chain Compounds*; Miller, J. S., Ed.; Plenum: New York, 1983; Vol. 3, p 143.
(10) Hatfield, W. E.; Estes, W. E.; Marsh, W. E.; Pickens, M. W.; ter Haar, L. W.; Weller, R. W. In *Extended Linear Chain Compounds*; Miller, J. S., Ed.; Plenum: New York, 1983; Vol. 3, p 43.
(11) Pei, Y.; Verdaguer, M.; Kahn, O.; Sletten, J.; Renard, J.-P. *J. Am. Chem. Soc.* **1986**, *108*, 7428.
(12) Coronado, E.; Drillon, M.; Fuertes, A.; Beltran, D.; Mosset, A.; Galy, J. *J. Am. Chem. Soc.* **1986**, *108*, 900.
(13) Preliminary results have been reported previously: Landee, C. P.; Djili, A. *Bull. Am. Phys. Soc.* **1986** *31*, 1155. Landee, C. P.; Djili, A.; Newhall, M.; Mudgett, D. F.; Willett, R. D.; Place, H.; Scott, B. In *Organic and Inorganic Low Dimensional Crystalline Materials*; Drillon, M., Delhaes, P., Eds.; NATO ASI Series; Plenum: New York; in press.
(14) Galbraith Laboratories, Knoxville, TN 37921.
(15) Landee, C. P.; Greeney, R. E. *Inorg. Chem.* **1986**, *25*, 3771.
(16) Wong, H.; tom Dieck, H.; O'Conner, C. J.; Sinn, E. *J. Chem. Soc., Dalton Trans.* **1980**, 786. Jones, D. H.; Sams, J. R.; Thompson, R. C. *Inorg. Chem.* **1983**, *22*, 1399.
(17) Swank, D. D.; Landee, C. P.; Willett, R. D. *Phys. Rev. B: Condens. Matter* **1979**, *20*, 2154.
(18) Swank, D. D.; Needham, G. F.; Willett, R. D. *Inorg. Chem.* **1979**, *18*, 761.
(19) Campana, C. F.; Shephard, D. F.; Litchman, W. M. *Inorg. Chem.* **1981**, *20*, 4039.
(20) Sheldrick, G. "SHELXTL"; Nicolet Analytical Instruments: Madison, WI, 1984.

Table I. X-ray Data Collection Parameters

compd name	tetrakis(tetramethylene sulfoxide)copper(II) hexabromodicuprate(II)	tetrakis(tetramethylene sulfoxide)copper(II) hexachlorodicuprate(II)
empirical formula	$C_{16}H_{32}O_4S_4Cu_3Br_6$	$C_{16}H_{32}O_4S_4Cu_3Cl_6$
diffractometer system	Nicolet R3m/E	Nicolet R3m/E
cryst class	triclinic	triclinic
space group	$P\bar{1}$	$P\bar{1}$
systematic absences	none	none
lattice consts		
a, Å	8.448 (2)	8.250 (4)
b, Å	9.630 (2)	9.330 (5)
c, Å	11.655 (2)	11.131 (6)
α, deg	65.42 (1)	67.59 (4)
β, deg	71.59 (2)	73.29 (6)
γ, deg	73.52 (1)	74.67 (6)
V, Å^3	805.2 (3)	747.0 (9)
	based on 25 reflcns in the range $28 < \theta < 30°$	based on 25 reflcns in the range $22 < \theta < 27°$
$F(000)$	520.90	412.94
radiation	Mo Kα with Zr filter	Mo Kα with Zr filter
cryst size, mm^3	0.2 × 0.15 × 0.1	0.25 × 0.42 × 0.50
abs coeff, cm^{-1}	96.18	29.58
calcd density, g cm^{-3}	2.22 (Z = 1)	1.82 (Z = 1)
type of abs cor	empirical ψ scan	empirical ψ scan
max, min transmssn	0.321, 0.235	0.850, 0.646
scan range, deg	1.0	1.0
min, max scan speed, deg min^{-1}	3.9, 29.30	3.9, 29.30
hkl check reflcns	100, 010, 002; monitored every 100 reflcns	111, 323; monitored every 100 reflcns
total no. of reflcns	1988	4645
2θ(max), deg	45	60
no. of unique reflcns	1878; 1483 with $I > 3\sigma$	4348; 3695 with $I > 3\sigma$
R for equiv reflcns	0.0190	0.0127
struct soln package	Nicolet SHELXTL	Nicolet SHELXTL
struct soln technique	direct methods	direct methods
$R = \sum\|\|F_o\| - \|F_c\|\|/\sum\|F_o\|$	0.0353	0.0377
$R_w = [\sum w(\|F_o\| - \|F_c\|)^2/\sum w\|F_o\|^2]^{1/2}$ with $w = 1/[\sigma^2(F) + g(F)^2]$; g	0.0403; 0.000 10	0.0456; 0.000 22
$\|1/\sigma\|$ max, mean	0.159, 0.033	0.026, 0.192
total no. of params refined	152	152
thermal params	anisotropic on all non-hydrogen atoms	anisotropic on all non-hydrogen atoms
hydrogen atoms	constrained to C–H and N–H = 0.96 Å; thermal params fixed at 0.10	constrained to C–H and N–H = 0.96 Å; thermal params fixed at 0.10
largest peak on final diff map, e Å^{-3}	0.62, near Br(3)	0.7, near Cl(3)
extinction cor	none	0.004 09
goodness of fit	1.386	1.700

structure factors for both compounds have been deposited as supplementary material.

Magnetic Measurements. The magnetic susceptibilities of powdered samples of the title compounds have been measured between 1.4 and 300 K in a PAR Model 155 vibrating-sample magnetometer. The temperatures above 1.8 K were determined by using a carbon-glass resistance thermometer that had been calibrated in situ against a commercially calibrated diode and magnetic standards.[21] Temperatures below 1.8 K were determined by using the vapor pressure[22] of ^{4}He. The magnetic field

(21) Landee, C. P.; Greeney, R. E.; Lamas, A. C. *Rev. Sci. Instrum.* **1987**, *58*, 1957.

Table II. Atomic Coordinates (×10^4) and Isotropic Thermal Parameters (Å^2 × 10^3) for Tetrakis(tetramethylene sulfoxide)copper(II) Hexabromodicuprate(II)

atom	x	y	z	U^a
Cu(1)	10 216 (1)	3859 (1)	−3433 (1)	45 (1)
Cu(2)	10 000	5000	0	43 (1)
Br(1)	8 369 (1)	4055 (1)	−1507 (1)	58 (1)
Br(2)	12 123 (1)	1629 (1)	−2661 (1)	67 (1)
Br(3)	10 057 (2)	6584 (1)	−4723 (1)	78 (1)
O(1)	11 434 (7)	2968 (6)	449 (6)	51 (3)
O(2)	8 227 (6)	4196 (6)	1491 (5)	47 (3)
S(1)	10 632 (3)	1488 (3)	1133 (2)	48 (1)
S(2)	6 327 (3)	4716 (3)	1512 (2)	46 (1)
C(24)	5 567 (11)	2935 (11)	2116 (10)	60 (6)
C(23)	5 323 (16)	2290 (14)	3539 (12)	102 (8)
C(22)	5 553 (16)	3329 (18)	4033 (10)	101 (9)
C(21)	5 443 (11)	4952 (12)	3046 (10)	66 (6)
C(14)	12 385 (13)	28 (10)	848 (10)	72 (6)
C(13)	13 275 (21)	−438 (21)	1848 (18)	181 (16)
C(12)	12 467 (20)	52 (17)	2887 (14)	122 (10)
C(11)	10 702 (15)	862 (11)	2775 (9)	74 (6)

[a] The equivalent isotropic U is defined as one-third of the trace of the orthogonalized U_{ij} tensor.

Table III. Atomic Coordinates (×10^4) and Isotropic Thermal Parameters (Å^2 × 10^3) for Tetrakis(tetramethylene sulfoxide)copper(II) Hexachlorodicuprate(II)

atom	x	y	z	U^a
Cu(1)	10 229 (1)	3928 (1)	−3443 (1)	39 (1)
Cu(2)	10 000	5000	0	35 (1)
Cl(1)	8 448 (1)	4100 (1)	−1570 (1)	49 (1)
Cl(2)	12 085 (1)	1828 (1)	−2704 (1)	62 (1)
Cl(3)	9 796 (2)	6538 (1)	−4655 (1)	72 (1)
O(1)	11 415 (2)	2917 (2)	488 (2)	44 (1)
O(2)	8 174 (2)	4222 (2)	1517 (2)	43 (1)
S(1)	10 559 (1)	1447 (1)	1101 (1)	41 (1)
S(2)	6 249 (1)	4739 (1)	1492 (1)	40 (1)
C(24)	5 510 (4)	2913 (4)	1966 (3)	53 (1)
C(23)	5 313 (6)	2160 (5)	3465 (4)	83 (2)
C(22)	5 613 (5)	3216 (5)	4050 (3)	74 (2)
C(21)	5 333 (4)	4895 (4)	3113 (3)	57 (2)
C(14)	12 303 (5)	−69 (4)	795 (4)	61 (1)
C(13)	13 379 (7)	−438 (7)	1737 (6)	116 (4)
C(12)	12 343 (7)	−221 (7)	2964 (5)	120 (3)
C(11)	10 605 (5)	756 (4)	2824 (3)	64 (2)

[a] The equivalent isotropic U is defined as one-third of the trace of the orthogonalized U_{ij} tensor.

Table IV. Bond Angles (deg) and Bond Distances (Å) in Tetrakis(tetramethylene sulfoxide)copper(II) Hexabromodicuprate(II)

	A. Lengths		
Cu(1)–Br(1)	2.341 (1)	Cu(1)–Br(2)	2.316 (1)
Cu(1)–Br(3)	2.410 (1)	Cu(1a)–Br(3)	2.447 (2)
C(2)–Br(1)	3.063 (1)	Cu(2)–Br(1a)	3.063 (1)
Cu(2)–O(1)	1.942 (5)	Cu(2)–O(2)	1.939 (5)
S(1)–O(1)	1.545 (6)	S(2)–O(2)	1.535 (6)
S(1)–C(11)	1.767 (11)	S(1)–C(14)	1.782 (9)
S(2)–C(21)	1.789 (12)	S(2)–C(24)	1.784 (11)
C(11)–C(12)	1.492 (19)	C(12)–C(13)	1.389 (27)
C(14)–C(13)	1.432 (26)	C(21)–C(22)	1.504 (16)
C(22)–C(23)	1.425 (26)	C(23)–C(24)	1.476 (16)
	B. Angles		
Cu(1)–Br(3)–Cu(1a)	91.1 (1)	Cu(1)–Br(1)–Cu(2)	112.4 (1)
Br(1)–Cu(1)–Br(2)	101.7 (1)	Br(1)–Cu(1)–Br(3)	98.8 (1)
Br(1)–Cl(1)–Br(3a)	134.9 (1)	Br(2)–Cu(1)–Br(3a)	98.5 (1)
Br(2)–Cu(1)–Br(3)	142.0 (1)	Br(3)–Cu(1)–Br(3a)	88.9 (1)
Br(1)–Cu(2)–O(1)	90.2 (2)	Br(1)–Cu(2)–O(2)	86.3 (2)
O(1)–Cu(2)–O(2)	89.8 (2)	O(1)–Cu(2)–O(2a)	90.1 (2)
O(1)–S(1)–C(11)	105.0 (5)	O(1)–S(1)–C(14)	102.2 (4)
C(11)–S(1)–C(14)	92.3 (5)	Cu(2)–O(1)–S(1)	120.1 (3)
Cu(2)–O(2)–S(2)	123.9 (3)	O(2)–S(2)–C(21)	102.8 (4)
O(2)–S(2)–C(24)	103.6 (4)	C(21)–S(2)–C(24)	91.2 (5)
S(2)–C(21)–C(22)	105.0 (9)	C(21)–C(22)–C(23)	110.5 (11)
C(22)–C(23)–C(24)	112.6 (10)	S(2)–C(24)–C(23)	108.4 (10)
S(1)–C(11)–C(12)	107.4 (8)	C(11)–C(12)–C(13)	109.8 (15)
C(12)–C(13)–C(14)	117.3 (14)	S(1)–C(14)–C(13)	106.3 (11)

Table V. Bond Angles (deg) and Bond Distances (Å) in Tetrakis(tetramethylene sulfoxide)copper(II) Hexachlorodicuprate(II)

	A. Lengths		
Cu(1)–Cl(1)	2.213 (1)	Cu(1)–Cl(2)	2.183 (1)
Cu(1)–Cl(3)	2.278 (1)	Cu(1)–Cl(3a)	2.325 (1)
Cu(2)–Cl(1)	2.894 (1)	Cu(2)–Cl(1a)	2.894 (1)
Cu(2)–O(1)	1.947 (2)	Cu(2)–O(2)	1.957 (2)
S(1)–O(1)	1.539 (2)	S(2)–O(2)	1.537 (2)
S(1)–C(11)	1.783 (4)	S(1)–C(14)	1.787 (3)
S(2)–C(21)	1.791 (4)	S(2)–C(24)	1.798 (4)
C(11)–C(12)	1.495 (7)	C(12)–C(13)	1.444 (8)
C(14)–C(13)	1.450 (8)	C(21)–C(22)	1.515 (5)
C(22)–C(23)	1.472 (8)	C(23)–C(24)	1.521 (5)
	B. Angles		
Cu(1)–Cl(3)–Cu(1a)	93.4 (1)	Cu(1)–Cl(1)–Cu(2)	112.3 (1)
Cl(1)–Cu(1)–Cl(2)	101.4 (1)	Cl(1)–Cu(1)–Cl(3)	97.4 (1)
Cl(1)–Cu(1)–Cl(3a)	138.9 (1)	Cl(2)–Cu(1)–Cl(3a)	96.5 (1)
Cl(2)–Cu(1)–Cl(3)	146.8 (1)	Cl(3)–Cu(1)–Cl(3a)	86.6 (1)
Cl(1)–Cu(2)–O(1)	90.8 (1)	Cl(1)–Cu(2)–O(2)	87.5 (1)
O(1)–Cu(2)–O(2)	89.2 (1)	O(1)–Cu(2)–O(2a)	89.2 (1)
O(1)–S(1)–C(11)	105.2 (2)	O(1)–S(1)–C(14)	102.5 (1)
C(11)–S(1)–C(14)	91.9 (2)	Cu(2)–O(1)–S(1)	119.6 (1)
Cu(2)–O(2)–S(2)	123.7 (1)	O(2)–S(2)–C(21)	102.1 (1)
O(2)–S(2)–C(24)	103.6 (1)	C(21)–S(2)–C(24)	91.6 (2)
S(2)–C(21)–C(22)	104.4 (3)	C(21)–C(22)–C(23)	109.0 (3)
C(22)–C(23)–C(24)	111.1 (3)	S(2)–C(24)–C(23)	107.5 (3)
S(1)–C(11)–C(12)	106.9 (3)	C(11)–C(12)–C(13)	113.2 (4)
C(12)–C(13)–C(14)	110.1 (4)	S(1)–C(14)–C(13)	107.3 (3)

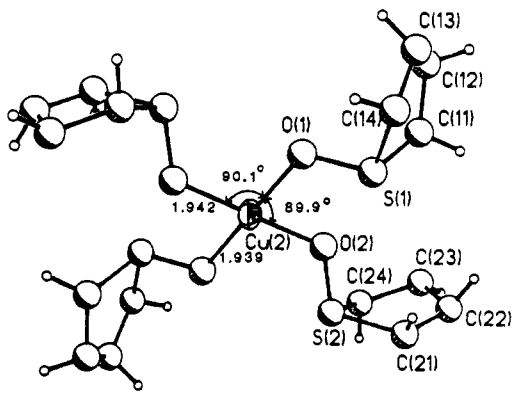

Figure 1. View of the cation of $CuBr_2 \cdot {}^4/_3TMSO$. Bond distances and angles are in units of angstroms and degrees, respectively.

was measured by using a Hall probe. The susceptibilities per mole of copper ions were corrected[23] for diamagnetism (-161×10^{-6} emu/mol, Br; -128×10^{-6} emu/mol, Cl) and temperature-independent paramagnetism of the cupric ion ($+60 \times 10^{-6}$ emu/mol).

Results and Discussion

Structural Description. The structures of the two title compounds are identical, consisting of chains of tetrakis(tetramethylene sulfoxide)copper(II) cations (Figure 1) and dimeric dibridged $Cu_2X_6^{2-}$ anions (Figure 2) that extend along the crystallographic *c* axis. The chains are well separated by the bulk of the TMSO groups (Figure 3), which prevent any copper–copper contacts shorter than the unit cell translation along the *a* axis (8.448 Å, Br; 8.250 Å, Cl). The figures contain bond distances and angles for the bromide; corresponding values for the chloride may be found in Table V.

The coordination geometry of the Cu(2) atom in the cation is a 4 + 2 configuration (Figure 1). The four oxygens are arranged around the copper in a square plane, with all of the angles being very nearly 90°. The two independent Cu–O distances are essentially equal, at 1.939 (5) and 1.942 (5) Å in the bromide, while two distinct values are observed in the chloride, Cu–O(1) = 1.947 (2) Å and Cu–O(2) = 1.957 (2) Å. The Cu(2) atom is also linked to the X(1) atom on the anion via longer Cu–X semicoordinate bonds, the Cu(2)–Br(1) distance being 3.062 Å and Cu(2)–Cl(1) being 2.894 Å. Through symmetry, the Cu(2) atom is also coordinated to the X(1a) atom on a second anion, yielding the common 4 + 2 coordination associated with copper(II) chemistry (Figure 2). The unit cell hence contains three copper ions, with one monomeric and one dimeric species. The semicoordinate bonds link these into alternating monomeric–dimeric chains running parallel to the *c* direction (Figure 3).

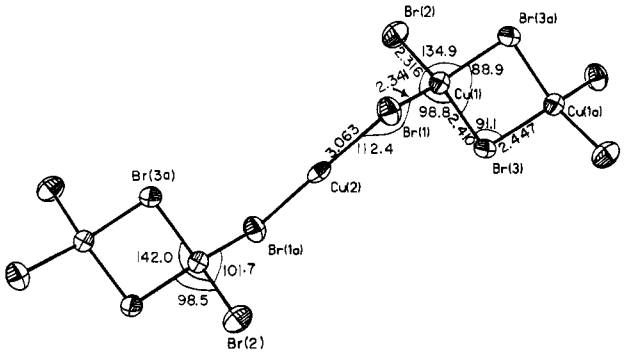

Figure 2. View of the chains of $Cu_2Br_6^{2-}$ anions and $Cu(TMSO)_4^{2+}$ cations in tetrakis(tetramethylene sulfoxide)copper(II) hexabromodicuprate(II). For clarity, the four TMSO groups around Cu(2) are omitted. The perspective is such that the Cu(1)–Cu(1a)–Br(3)–Br(3a) plane lies in the plane of the page. Bond distances and angles are given in units of angstroms and degrees, respectively.

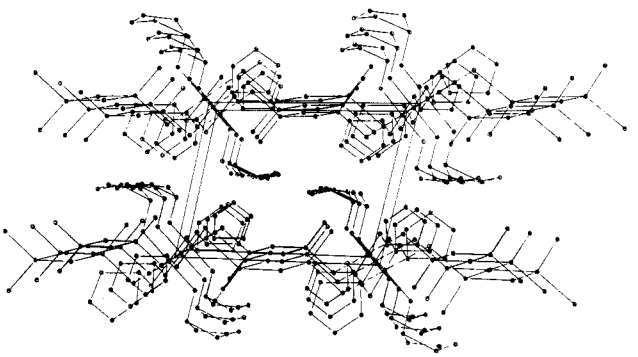

Figure 3. Crystal packing in tetrakis(tetramethylene sulfoxide)copper(II) hexachlorodicuprate(II). The chains extend along the *c* axis to the right of the diagram. The *a* and *b* axes point to the top and into the page, respectively.

The geometry around the Cu(1) atom (Figure 2) is intermediate between square planar and tetrahedral. The average terminal Cu–X distances are approximately 0.10 Å shorter than the average bridging Cu–X distances with 2.198 Å vs 2.302 Å (Cl) and 2.329 Å vs 2.429 Å (Br). In both cases, the Cu–Br distances are about 0.13 Å longer than the corresponding Cu–Cl distances, in accordance with the difference in ionic radii of the two halide ions (1.95 Å, Br^-; 1.80 Å; Cl^-). The average trans angles X–Cu(1)–X are 138.4° (Br) and 142.8° (Cl) where 109.5° would be associated with tetrahedral geometry and 180° with square planar. The magnetically important Cu(1)–X(3)–Cu(1) bridging angles are 91.1° for the bromide and 93.4° for the chloride. These changes represent interesting systematic variations between the geometries of the $Cu_2Cl_6^{2-}$ and $Cu_2Br_6^{2-}$ species, which are related to the difference in ionic radii of the two halide ions. Despite the increase in Cu–X distances, the X···X contact distances increase less than the increase in ionic radii (2×0.15 Å = 0.3 Å). Thus, the copper coordination geometry distorts more toward tetrahedral upon replacement of Cl^- by Br^-, leading to the 4.4° decrease in the trans X–Cu–X angles. Similarly, the two bridging bromide ions are forced to move further away from the Cu–Cu line, which consequently causes the bridging Cu–X–Cu angle to decrease 2.3°.

Structural Discussion. The present structure may be contrasted to that of $[CuL_3]Cu_2Cl_6 \cdot (CH_3)_2CO$, where L = $Ph_2P(O)CH_2P$-

(22) *NBS Monogr. (U.S.)* 1960, *No. 10.*
(23) Selwood, P. W. *Magnetochemistry*, 2nd ed.; Interscience: New York, 1956.

Table VI. Structural and Magnetic Properties of $Cu_2Cl_6^{2-}$ Dimers

compd	ref	terminal Cu–Cl (av), Å	bridging Cu–Cl (av), Å	trans Cl–Cu–Cl (av), deg	bridging Cu–Cl–Cu (av), deg	τ, deg	J/k, K
$CuL_3Cu_2Cl_6 \cdot C_3H_6O$	*a*	2.203	2.300	143.2	92.9	50.8	
		2.181		124.8		77.2	
$Cu(TMSO)_4Cu_2Cl_6$	this work	2.198	2.302	142.8	93.4	51.0	20
Ph_4PCuCl_3	*b*	2.219	2.306	143.4	93.3	50	38
							56
$Ph_4AsCuCl_3$	*c*	2.206	2.319	144.9	93.7	48.2	28
$Ph_4SbCuCl_3$	*d*	2.200	2.313	147.6	94.6	44.4	63
(15-crownNa)$CuCl_3$	*e*	2.195	2.293	141.8	92.2	52.9	
(18-crownNa)$CuCl_3$	*e*	2.220	2.290	147.0	93.6	45.6	
(DBTTF)$CuCl_3$	*f*	2.224	2.297	173.2	96.2	≈0	−60
(morpholinium)$CuCl_3$	*g*	2.240	2.283	175.8	95.8	≈0	−43

[a] Yatsimirskii, K. B.; Struchkov, Yu. t.; Batsanov, A. S.; Sinyauskaya, E. I. *Koord. Khim.* **1985**, *11*, 826. [b] Textor, M.; Dubler, E.; Oswald, H. R. *Inorg. Chem.* **1974**, *13*, 1361 (structure). Hanson, M. V.; Smith, C. B.; Carlisle, G. O., *Inorg. Nucl. Chem. Lett.* **1976**, *12*, 917 (susceptibility). Estes, W. E.; Wasson, J. R.; Hall, J. R.; Hall, J. W.; Hatfield, W. E. *Inorg. Chem.* **1978**, *17*, 3657 (susceptibility). [c] Chow, C.; Caputo, R.; Willett, R. D.; Gerstein, B. C. *J. Chem. Phys.* **1974**, *61*, 271 (susceptibility). Willett, R. D.; Chow, C. *Acta Crystallogr., Sect. B: Struct. Crystallogr. Cryst. Chem.* **1973**, *B30*, 207 (structure). [d] Bencini, A.; Gatteschi, D.; Zanchini, C. *Inorg. Chem.* **1985**, *24*, 704. [e] Dreissig, W.; Dauter, Z.; Cygan, A.; Biernat, J. F. *Inorg. Chim. Acta* **1985**, *96*, 21. [f] Honda, M.; Katayama, C.; Tanaka, J.; Tanaka, M. *Acta Crystallogr., Sect. C: Cryst. Struct.* **1985**, *C41*, 197. Tanaka, M.; Tanaka, J. Presented at the Molecular Structure Symposium, Tokyo, Sept 1985; paper 1P16. [g] Scott, B.; Geiser, U.; Willett, R. D.; Bonamartini-Corradi, A.; Battaligia, L.; Pellacani, G. C.; Manfredini, T., to be submitted for publication.

(O)Ph_2.[24] This compound contains discrete CuL_3^{2+} cations, $Cu_2Cl_6^{2-}$ anions, and lattice acetone molecules. The $Cu_2Cl_6^{2-}$ dimeric species does not contain a center of inversion, and the coordination spheres about the two copper atoms exhibit different amounts of tetrahedral distortion. The twist angles, τ, are 50.8 and 77.2°, respectively, where τ is defined as the angle between the central Cu_2X_2 core and the terminal CuX_2 plane.[25] The latter represents the largest twist angle observed in $Cu_2Cl_6^{2-}$ dimers and one of the largest known in copper(II) halide salts. (The value of τ in the antiferromagnetic $(CuBr_2)_n$ chain in (Et_2NH_2)-$Cu_3Br_8 \cdot CuBr_2 \cdot EtOH$ is 86°.[26])

The structure of $Cu_3Cl_6(C_6H_7NO)_2 \cdot 2H_2O$ is similar to that of the $CuX_2 \cdot {}^4/_3TMSO$ compounds and contains planar $CuCl_2(H_2O)_2$ moieties and *N*-oxide-bridged $Cu_2(C_6H_7NO)_2Cl_4$ dimers linked together into chains by semicoordinate bonds, analogous to the structure of the TMSO salts reported here. Strong antiferromagnetic coupling within the dimers dominates the magnetic behavior.[27]

Trimer copper(II) halide salts containing planar, dibridged $Cu_3X_6L_2$, $Cu_3X_7L^-$, or $Cu_3X_8^{2-}$ anions are known for a wide variety of systems.[28] These stack via formation of semicoordinate Cu···X bonds between trimers to form infinite chains. These semicoordinate bonds yield a pseudofrustrated magnetic ground state for the chains. The magnetic behavior of oligomeric systems of this type has recently been reviewed.[29] An isolated $Cu_3Cl_{14}^{8-}$ ion exists in $(C_6N_3H_{18})Cu_5Cl_{22}$,[30] consisting of a square-planar $CuCl_4^{2-}$ ion linked via semicoordinate bonds to the apical chloride ions on two square-pyramidal $CuCl_5^{3-}$ ions. Two isolated distorted-tetrahedral $CuCl_4^{2-}$ anions also exist in the lattice.

The compound $3CuCl_2 \cdot 2$(dioxane) contains dibridged chains with three copper(II) ions in the repeat unit.[31] The exchange pathways are specified by a repeat sequence J_F, J_F, J_{AF} with $J_F \gg |J_{AF}|$.[32] This sequence yields an $S = 0$ ground state for the chain. The system $(C_5N_5H_6)_2Cu_3Cl_8 \cdot 4H_2O$ contains chains of trimers with antiferromagnetic coupling within the trimers and weaker, perhaps negligible, coupling between trimers.[33]

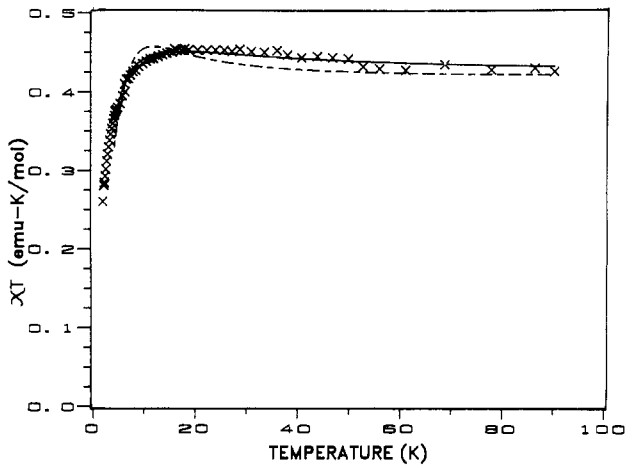

Figure 4. Magnetic susceptibility per mole of copper ions of $CuBr_2 \cdot {}^4/_3TMSO$ plotted as the product χT versus temperature. The solid line corresponds to the theoretical prediction for the data based on the isolated trimer model, eq 2, using best fit parameters $J_d/k = 12$ K and $J_m/k = -1.5$ K with g fixed at 2.12. The dashed line corresponds to the best fit to the molecular field corrected dimer plus monomer model, eq 1, with best fit parameters $J_d/k = -11$ K and $\Theta = -11.2$ K.

Unusual chains exist in $[(CH_3)_2CHNH_3]CuCl_4$, containing square-planar $CuCl_4^{2-}$ ions (site 1) linked (via semicoordinate bonds) to pairs of distorted-tetrahedral $CuCl_4^{2-}$ ions (sites 2 and 3).[34] Thus the repeating exchange pathways along the chain are specified by J_{12}, $J_{21'}$, J_{13}, and $J_{13'}$. The magnetic susceptibility[35] and EPR spectra[36] have been reported. A wide variety of other trimeric copper(II) systems are known,[37] including chains of trimers.[38]

(24) Yatsimirskii, K. B.; Struchkov, Yu. T.; Batsanov, A. S.; Sinyauskaya, E. I. *Koord. Khim.* **1985**, *11*, 826.
(25) Willett, R. D. In *Magneto-Structural Correlations in Exchange Coupled Systems*; Willett, R. D., Gatteschi, D., Kahn, O. Eds.; NATO ASI Series; Plenum: New York, 1985; p 389.
(26) Fletcher, R.; Hansen, J. J.; Livermore, J.; Willett, R. D. *Inorg. Chem.* **1983**, *22*, 330.
(27) Sager, R. S.: Watson, W. H. *Inorg. Chem.* **1968**, *7*, 2035. Whyman, R.; Hatfield, W. E. *Inorg. Chem.* **1967**, *6*, 1859.
(28) Grigereit, T.; Ramakriska, B. L.; Place, H.; Willett, R. D.; Pellacani, G. C.; Manfredini, T.; Menabue, L.; Bonamartini-Corradi, A.; Battaglia, L. P. *Inorg. Chem.* **1987**, *26*, 2235 and references therein. Bond, M., private communication.
(29) Willett, R. D.; Grigereit, T.; Halvorson, K.; Scott, B. *Proc. Indian Acad Sci.* **1987**, *98*, 147.
(30) Antolini, L.; Marcotrigiano, G.; Menabue, L.; Pellacani, G. C. *J. Am. Chem. Soc.* **1980**, *102*, 5506.
(31) Barnes, J. C.; Weakley, T. J. R. *Acta Crystallogr., Sect. B: Struct. Crystallogr. Cryst. Chem.* **1977**, *B32*, 921.
(32) Livermore, J. C.; Willett, R. D.; Gaura, R. M.; Landee, C. P. *Inorg. Chem.* **1982**, *21*, 1403.
(33) de Meester, P.; Skapski, A. C. *J. Chem. Soc., Dalton Trans.* **1972**, 2408. Brown, D. B.; Wasson, J. R.; Hall, J. W.; Hatfield, W. E. *Inorg. Chem.* **1977**, *16*, 2526.
(34) Anderson, D. N.; Willett, R. D. *Inorg. Chim. Acta* **1974**, *8*, 167.
(35) Swank, D. D.; Landee, C. P.; Willett, R. D. *J. Magn. Magn. Mater.* **1980**, *15–18*, 319.
(36) Bloomquist, D. R.; Willett, R. D. *J. Phys. Chem. Solids* **1981**, *42*, 455.
(37) Journaux, Y.; Sletten, J.; Kahn, O. *Inorg. Chem.* **1986**, *25*, 439. Chiari, B.; Piovesana, B.; Tarantelli, T.; Zanazzi, P. F. *Inorg. Chem.* **1985**, *24*, 4615. Thompson, L. K.; Woon, T. C.; Murphy, D. B.; Gabe, E. J.; Lee, F. L.; LePage, Y. *Inorg. Chem.* **1985**, *24*, 4719.

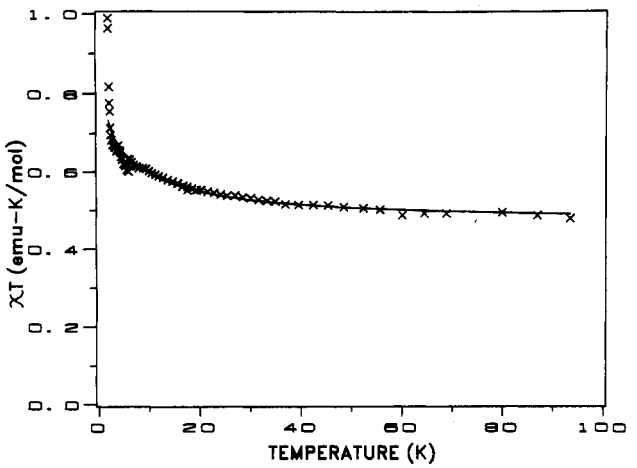

Figure 5. Magnetic susceptibility per mole of copper ions of $CuCl_2 \cdot {}^4/_3TMSO$ plotted as the product χT versus temperature. The solid line corresponds to the theoretical prediction for the data based on the isolated trimer model, eq 2, using best fit parameters J_d/k = 20 K and J_m/k = 1.6 K with g fixed at 2.17.

The geometry of the $Cu_2Cl_6^{2-}$ anion in the title compound is very similar to that observed in other salts containing this species, as summarized in Table VI. The average terminal Cu–Cl bond distances are in the range 2.181–2.219 Å, while the bridging distances are roughly 0.1 Å longer (2.300–2.319 Å average). The average trans Cl–Cu–Cl angles, with one exception, are in the range 142.8–147.6°, while the bridging Cu–Cl–Cu angles range from 92.9 to 94.6°. Also included in Table VI for comparison purposes are two isolated, planar $Cu_2Cl_6^{2-}$ dimers, (DBTTF)$CuCl_3$ and (morpholinium)$CuCl_3$.

Magnetic Results. Qualitative Analysis. The experimental data below 100 K, plotted as the product of χT versus temperature, are presented in Figures 4 and 5 for the bromide and chloride, respectively. These data correspond to the susceptibility per mole of copper atoms and hence correspond to the formula $CuX_2 \cdot {}^4/_3TMSO$. As the temperature is lowered, the product χT, proportional to the square of the effective moment, grows slowly, indicating dominant ferromagnetic interactions. Below 20 K the two compounds behave quite differently, the χT product of the bromide descending rapidly (Figure 4) while χT of the chloride ascends steeply (Figure 5). Even though χT of the bromide decreases rapidly, its susecptibility continues to increase as the temperature is lowered to 1.4 K and never shows a maximum. The change of behavior below 20 K indicates the onset of the influence of additional interactions.

The magnetic data above 60 K for both compounds have been analyzed in terms of the Curie–Weiss equation, $\chi = C/(T - \Theta)$, yielding values of the parameters for the chloride of C(Cl) = 0.44 (1) emu K/mol (g_{Cl} = 2.17 (1)) and Θ(Cl) = 7 (2) K, while the same analysis for the bromide yields C(Br) = 0.42(1) emu K/mol (g_{Br} = 2.12 (1) and Θ(Br) = 3 (1) K. The positive values found for the two Θ values signify the presence of dominant ferromagnetic interactions at higher temperatures within the two compounds.

Insight into the origin of the ferromagnetic interaction within these compounds is provided by referring to the results of recent studies on magnetostructural correlations. Superexchange within copper dimers is a well-studied phenomenon,[39] and the dependence of the sign and magnitude of the superexchange interaction upon structural parameters such as the bridging angle and the coordination geometry is becoming increasingly well characterized. As reported in a study of magnetic interactions within planar bridged copper chloride dimers,[40] ferromagnetic interactions are found when the Cu–Cl–Cl bridging angle is less than 95°. This basic result, which followed the earlier study on hydroxide-bridged dimers,[41] has been confirmed in a variety of other copper dimers and dibridged linear chains,[25] while the importance of folding and twisting of the superexchange network has also received attention.[42] It has also been recognized that ferromagnetic interactions, where they arise, have magnitudes that remain essentially unchanged upon substitution of chloride for bromide but that antiferromagnetic contributions are approximately twice as strong in bromide compounds as they are in the isostructural chlorides.[43] On the basis of this knowledge, the ferromagnetic interactions that dominate the high-temperature susceptibility for the two compounds are therefore attributed to a superexchange interaction between the two copper ions in the respective $Cu_2X_6^{2-}$ anions. This interaction strength will be characterized by the parameter J_d. The bridging angles of 91.1° (Br) and 93.4° (Cl) lie in the range where the ferromagnetic contribution to exchange is expected to dominate and the deviations from planarity are such as to predict ferromagnetic coupling for these dimeric species. Indeed, in those salts that contain isolated dimers (Table VI), ferromagnetic behavior is observed in the susceptibilities, corresponding to exchange strengths in the range J/k = 28–65 K. However, because of the strong correlation of J with both g and the value used for the temperature-independent paramagnetism (TIP) in these systems, the differences between the various exchange strengths cannot be regarded as significant.

Ferromagnetic exchange within a $S = {}^1/_2$ Heisenberg dimer causes the S = 1 triplet state to lie at an energy $2J$ below the nonmagnetic S = 0 singlet state; consequently, the product χT rises by one-third as the temperature decreases to zero and the fraction of dimers within the magnetic state increase from 75% to 100%. Such a gradual rise is seen in Figures 4 and 5 down to 20 K; below that temperature, the sharp decrease (Br) and rise (Cl) are not predicted by the isolated dimer model and must signify the influence of an additional interaction. It is not likely to arise from interactions between the chains, since the most direct copper–copper distance between chains is equal to the a-axis repeat distance, 8.448 Å (Br) and 8.250 Å (Cl), with no superexchange pathways evident that connect the chains (Figure 3). The second interaction is more likely to arise from superexchange between the Cu(1) sites and Cu(2) sites through the X(1) halides, characterized by a parameter J_m. Such interactions have been frequently observed in systems with stacked $Cu_nX_{2n+2}^{2-}$ oligomers[44] and other types of alternating-chain compounds.[1,39] They are generally weak when found in systems connected by long bonds such as the Cu(2)–X(1) bond of 3.063 Å (Br) and 2.894 Å (Cl). The existence of the inversion center at the Cu(2) site means the Cu(2) monomeric unit is magnetically connected equally to the Cu(1) atoms in two distinct dimers (Figure 2). The consequent superexchange pathway therefore extends indefinitely along the chain axis, involving a repeat pattern of three exchange strengths, two of which are identical by symmetry: $...J_dJ_mJ_mJ_dJ_mJ_m...$. Since antiferromagnetic interactions reduce χT while ferromagnetic exchange enhances the product, it is clear from the data below 20 K that J_m(Br) must be antiferromagnetic while J_m(Cl) is ferromagnetic.

Magnetic Quantitative Analysis. There exist no predictions in the literature for the susceptibility of an alternating $S = {}^1/_2$ Heisenberg chain involving three exchange strengths, even when two of them are identical. Alternating exchange in Heisenberg antiferromagnetic chains has been studied in detail[45] but only for

(38) Hulsbergen, F. B.; ten Holdt, R. W. M.; Verschoor, G. C.; Reedijk, J.; Spek, A. L. *J. Chem Soc., Dalton, Trans.* **1983**, 539. Knuuttila, H. *Inorg. Chim. Acta* **1981**, *50*, 221.

(39) For a review, see: Hatfield, W. E. In *Magneto-Structural Correlations in Exchange Coupled Systems*; Willett, R. D., Gatteschi, D., Kahn, O., Eds.; NATO ASI Series; Plenum: New York, 1985; p 555.

(40) Roundhill, S. G. N.; Roundhill, D. M.; Bloomquist, D. R.; Landee, C. P.; Willett, R. D.; Dooley, D. M.; Gray, H. B. *Inorg. Chem.* **1979**, *18*, 831.

(41) Crawford, V. H.; Richardson, H. W.; Wasson, J. R.; Hodgson, D. J.; Hatfield, W. E. *Inorg. Chem.* **1976**, *15*, 2107.

(42) Battaglia, L. P.; Corradi, M. B.; Geiser, U.; Willett, R. D.; Motori, A.; Franco, S.; Antolini, L.; Manfredini, T.; Menabue, L.; Pellacani, G. C. *J. Chem. Soc., Dalton Trans.*, in press.

(43) Willett, R. D. *Inorg. Chem.* **1986**, *25*, 1918.

(44) Geiser, U.; Willett, R. D.; Lindbeck, M.; Emerson, K. *J. Am. Chem. Soc.* **1986**, *108*, 1173.

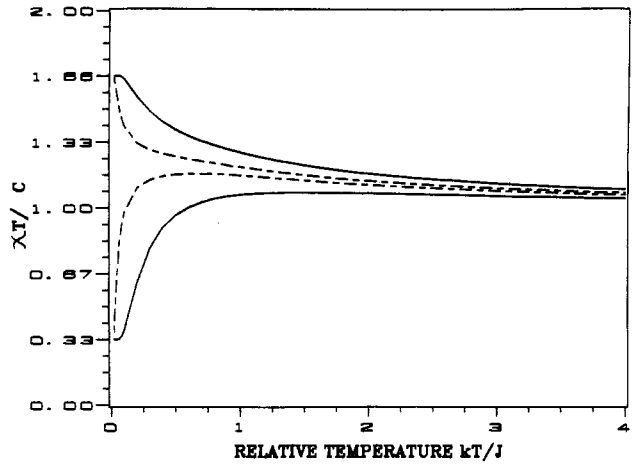

Figure 6. Reduced magnetic susceptibility $\chi T/C$ plotted versus the relative temperature kT/J_1 for the isolated trimer model of eq 2. J_1 is taken as positive and is larger than J_2. The upper and lower solid curves correspond to ratios J_2/J_1 of 0.25 and −0.25, respectively, while the upper and lower dashed curves correspond to the ratio of 0.05 and −0.05, respectively.

the case of purely antiferromagnetic interactions. These results are inapplicable since the J_d exchange in both title compounds is clearly ferromagnetic.

As a first approximation to the magnetic behavior, the data of the bromide have been compared to the prediction for a model of a $S = {}^1/_2$ Heisenberg dimer plus a paramagnetic monomer, with interoligomer interactions accounted for with a molecular field approximation. The susceptibility is given according to eq 1 where the Curie constants for the dimer and monomer are each

$$\chi_m = C(m)/(T - \Theta) + C(d)/(T - \Theta)[1 + 3\exp(-2J/kT)]^{-1} \quad (1)$$

based upon their own g factors. In order to avoid an excess of parameters, the g factors were held fixed at typical values, g(monomer) = 2.20 and g(dimer) = 2.08. These correspond to an average value of 2.12, consistent with the Curie constant for the bromide. The data below 90 K were compared to eq 1 with J and Θ as free parameters. A fair quantitative agreement was found with the data, although the parameters varied as a function of the range of data included. Results of the fit obtained for data between 4.5 and 90 K are shown as the dashed line in Figure 4; the derived parameters are $J/k = 11$ K and $\Theta = -11.2$ K. While the exchange strength seems plausible, the molecular field term is too large a fraction of J for this model to be considered reliable.

An alternative approach is to compare the data to the model of a linear Heisenberg trimer with two inequivalent exchange parameters, J_1 and J_2, and Hamiltonian $H = -2J_1S_1\cdot S_2 - 2J_2S_2\cdot S_3$. This model predicts[46] that the susceptibility per mole of copper atoms is given by the formula

$$\chi_m = (N\mu^2g^2/3T)(10e^{-A+B} + e^{-A-B} + e^{-A})/(2e^{-A+B} + e^{-A-B} + e^{-A}) \quad (2)$$

where $A = (J_1 + J_2)/kT$ and $B = (J_1^2 + J_2^2 - J_1J_2)^{1/2}/kT$. The predictions of this model, plotted as $\chi T/C$ versus the ratio kT/J_1, are shown in Figure 6 for several values of the ratio J_2/J_1. In this discussion, J_1 is taken as ferromagnetic and larger in magnitude than the other exchange strength. At high temperatures, J_1 dominates and the product χT increases with decreasing temperature for all J_2. For an antiferromagnetic J_2 interaction, the ground state is a doublet with one unpaired spin; the value of χT at low temperatures therefore approaches a constant value of $C/3$, where C is the Curie constant. The rate at which the limit is approached and the relative temperature at which the maximum of χT occurs depend on the ratio $|J_2/J_1|$; the two lower curves plotted in Figure 6 correspond to ratios of −0.25 and −0.05. When both exchange constants are ferromagnetic, χT always increases with decreasing temperature, approaching the limiting value corresponding to one $S = {}^3/_2$ entity at a rate corresponding to the ratio J_2/J_1.

It is recognized that this isolated trimer model cannot adequately represent the behavior of the extended chains found in the title compounds at temperatures that are comparable to the weaker of the two exchange strengths. Consider first the case in which the weaker of the exchange strengths is antiferromagnetic. Within each unit cell, there is a partial cancellation of the moments, reducing the number of independent spins from 3 to 1. Nevertheless, since the unit cells are connected together by the weak antiferromagnetic exchange, a, the single remaining spin within each unit cell is aligned parallel to the resultant spin of the neighboring unit cells and the chain is reduced to a $S = {}^1/_2$ ferromagnetic linear chain, for which it is known[47] that χT diverges as $T^{-0.7}$. In the event that the weaker of the exchange strengths is also ferromagnetic, b, the effective $S = {}^3/_2$ units are coupled by the J_2 into a $S = {}^3/_2$ ferromagnetic chain for which χT will diverge at even a faster rate. These ferrimagnetic divergences will only occur at temperatures that are low compared to the weaker of the exchange strengths but are completely different from the limiting behavior seen in the isolated trimers.

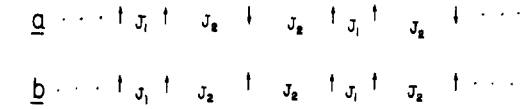

The data for $CuBr_2\cdot{}^4/_3TMSO$ have been compared to the predictions of the trimer model. With g held fixed at a value of 2.12, corresponding to the Curie constant determined by the Curie–Weiss fit, the data above 4 K are described well with best fit parameters of $J_1 = 12 \pm 4$ K and $J_2 = -3.0 \pm 0.2$ K, as shown with the solid line in Figure 4. Attempts to include lower temperature data in the fit led to equally good agreement between data and model but with systematic shifts in the parameters; this is to be expected as explained in the above paragraph. The ferromagnetic exchange J_1 is identified with the exchange strength within the dimers J_d. The other exchange constant, J_2, must correspond to the two interactions J_m between the monomeric copper atom and its two neighboring dimers, so we conclude $J_m = {}^1/_2J_2 = -1.5 \pm 0.1$ K. When all three parameters J_1, J_2, and g are allowed to vary independently, the best fit values are $J_1 = 25 \pm 4$ K, $J_2 = -2.5 \pm 0.2$ K, and $g = 2.06 \pm 0.005$, demonstrating the strong correlation between a ferromagnetic exchange and the g factor.

The results of applying the independent trimer model to the chloride compound are shown as the solid line in Figure 5, where the best fit parameters were found to be $J_1/k = 16 \pm 3$ K, $J_2/k = 2.5 \pm 0.4$ K, and $g = 2.20 \pm 0.02$ ($C = 0.45$). When g is held fixed at 2.17, corresponding to the Curie–Weiss constant, the parameters change to $J_1/k = 20 \pm 3$ K and $J_2/k = 3.2 \pm 0.4$ K but give a nearly equivalent fit. Disagreement between the model and data appeared at a higher temperature for the chloride than for the bromide case, which is attributed to the divergence in the chloride susceptibility. While the trimer model always predicts a finite low-temperature limit for χT, the bromide data also stay finite, but the chloride data increase without limit. As in the bromide case, J_d is taken as the stronger of the two exchanges, J_1, and J_m equals half of the weaker exchange interaction, J_m(Cl) = 1.6 K.

Magnetic Discussion. Two examples of $S = 1$, $S = {}^1/_2$ ferrimagnetic chains have been previously reported, both involving alternating chains of copper and nickel ions. The first,[48] CuNi(oxalato)·$4H_2O$, was not obtained as single crystals, but EXAFS studies suggest an ordered bimetallic chain in which each

(45) Duffy, W.; Barr, K. P. *Phys. Rev.* **1968**, *165*, 647. Hall, J. W.; Marsh, W. E.; Weller, R. R.; Hatfield, W. E. *Inorg. Chem.* **1981**, *20*, 1033.
(46) Sinn, E. *Coord. Chem. Rev.* **1970**, *5*, 313.
(47) Bonner, J. C.; Fisher, M. E. *Phys. Rev. A* **1964**, *A135*, 640.
(48) Verdaguer, M.; Julve, M.; Michalowicz, A.; Kahn, O. *Inorg. Chem.* **1983**, *22*, 2624.

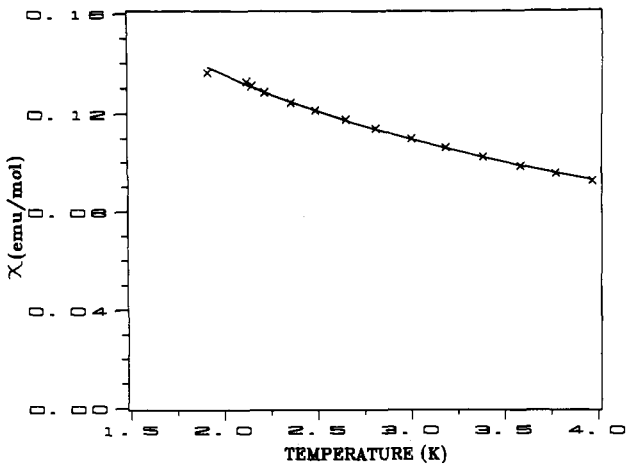

Figure 7. Magnetic susceptibility per mole of copper ions of $CuBr_2 \cdot {}^4/_3TMSO$ plotted as susceptibility versus temperature. The solid line corresponds to the theoretical prediction for the data based on eq 3 for the susceptibility of a $S = {}^1/_2$, $S = 1$ ferrimagnetic chain. The best fit parameters correspond to an antiferromagnetic exchange between adjacent $S = {}^1/_2$ ions of $J/k = -0.94$ K.

nickel ion is surrounded by six oxygen atoms as nearest neighbors (four from oxalate groups; two from water molecules), while the copper atoms are surrounded by four oxygens from the oxalate groups as well as two copper atoms from adjacent chains, about 4 Å distant. The magnetic susceptibility corresponded to an antiferromagnetic chain with an exchange strength $J/k = -38$ K (based on a Hamiltonian $H = -2J\sum S_i \cdot S_{i+1}$), but the characteristic minimum in χT was not observed. This was attributed to the amount of interaction between the chains.

Better linear-chain isolation was found in the NiCu ordered bimetallic $NiCu(pba)(H_2O)_3 \cdot 2H_2O$[5], in which the shortest separation between metal atoms belonging to neighboring chains is 5.21 Å. The magnetic data show the characteristic minimum in χT at 83 K. The divergence of χT in the low-temperature end is stopped by the onset of long-range antiferromagnetic order near 7 K.

An expression has been developed[49] for the susceptibility of a $S = {}^1/_2$, $S = 1$ antiferromagnetic chain, based on numerical analysis of such finite chains. The resulting expression for the magnetic susceptibility, expressed as a polynomial ratio, is

$$\chi_m = (N\mu^2g^2/kT)(AX + BX^2 + CX^3 + 11)/(DX^2 + EX + 12) \quad (3)$$

where $A = -0.034\,146\,801$, $B = 2.816\,930\,641\,1$, $C = -7.231\,001\,369\,7$, $D = 1.296\,632\,74$, $E = 0.697\,190\,135\,95$, and $X = |2J|/kT$. This model is appropriate for $CuBr_2 \cdot {}^4/_3TMSO$ since the trimer model indicates the dimeric coppers are locked into a $S = 1$ triplet state at temperatures small compared to $2J_d/k$ or 24 K, and the interaction between the dimeric coppers and the monomeric copper in the bromide is antiferromagnetic. (Equation 3 cannot be applied to the chloride since $J_m(Cl)$ is ferromagnetic.) Comparison of the bromide data below 6 K to the expression above predicts $|J/k| = 0.47$ K with $g = 1.22$. This magnitude for the exchange strength can not be compared to $J_m(Br)$ directly since the model for which the above expression was derived assumed an interaction between a $S = {}^1/_2$ and a $S = 1$ unit, while in $CuBr_2 \cdot {}^4/_3TMSO$ the interacting ions are both $S = {}^1/_2$. Comparing interaction strengths as $-2Js \cdot S = -2J_m s \cdot s$, where $s = {}^1/_2$ and $S = 1$, we see that, for $J/k = -0.47$ K, the corresponding $J_m/k = -0.94$ K. This is in reasonable agreement with the value of $J_m(Br)$ found as -1.50 K on the basis of the approximate trimer model. The expression above predicts that the minimum in χT is found near $0.7|J/k|$ or near 0.65 K for the bromide compound. Experiments are planned at lower temperatures to search for this minimum.

The values of J_d obtained for **1** and **2** are in reasonable accord with those observed in other twisted $Cu_2X_6^{2-}$ systems,[25,29] considering the errors associated with the determination of ferromagnetic exchange constants. The results corroborate the intiutive qualitative argument, as well as theoretical calculations,[50] that the antiferromagnetic contribution to the exchange decreases as the overlap between the individual magnetic orbitals decreases. This is particularly clearly pointed out by comparison with the magnetic results for the isolated planar dimers listed in Table VI. The change in sign of J_m upon replacement of Br^- by Cl^- is somewhat more difficult to understand. Simple overlap arguments predict this interaction should be ferromagnetic, since the long semicoordinate Cu(2)–X(1) bond is normal to the CuO_4 plane of the monomer, thus giving zero overlap between the unpaired electron on the dimeric copper and the Cu $d(x^2 - y^2)$ orbital. This is consistent with the behavior of **2**. The antiferromagnetic value for J_m in **1** may be associated with an overlap of the dimer orbitals with the ligand orbitals on the monomer. The Cu(1)–X(1)–S(2) angle is nearly linear, and the X(1)–S(2) nonbonded distance is small (Br(1)–S(2) = 3.629 Å; Cl(1)–S(2) = 3.561 Å). Since the increase in bond length (less than 0.07 Å) upon replacement of Cl^- by Br^- is less than the change in ionic radii (0.15 Å), this pathway could provide the necessary antiferromagnetic contribution to the exchange. A similar pathway has been identified as leading to antiferromagnetic exchange in $CuCl_2 \cdot DMSO$.[17]

Acknowledgment. This work was supported in part by the National Science Foundation under Grants DMR-8306432 (C.P.L.) and DMR-8219430 (R.D.W.). The magnetometer was purchased with a grant from the NSF College Research Instrumentation Program. R.D.W. acknowledges the support of The Boeing Co. and NSF Grant CHE-8408407 in acquiring the Nicolet R3m/E automated diffractometer system. We thank Dr. E. Coronado for making available his results for the susceptibility of the ferrimagnetic chain and Robert Greeney for his assistance with the magnetic data collection.

Registry No. $[Cu(TMSO)_4][Cu_2Cl_6]$, 14522-98-6; $[Cu(TMSO)_4][Cu_2Br_6]$, 14481-13-1.

Supplementary Material Available: Tables 7S and 8S, listing anisotropic thermal parameters for $CuBr_2 \cdot {}^4/_3TMSO$ and $CuCl_2 \cdot {}^4/_3TMSO$, respectively, and Tables 9S and 10S, listing the hydrogen atom positions and isotropic thermal parameters for $CuBr_2 \cdot {}^4/_3TMSO$ and $CuCl_2 \cdot {}^4/_3TMSO$, respectively (2 pages); tables of calculated and observed structure factors for $CuBr_2 \cdot {}^4/_3TMSO$ and $CuCl_2 \cdot {}^4/_3TMSO$ (37 pages). Ordering information is given on any current masthead page.

(49) Coronado, E., private communication.

(50) Hay, P. C.; Thiebault, J. C.; Hoffmann, R. *J. Am. Chem. Soc.* **1975**, *97*, 4884.